Nonlinear Response in Nanoshear Modulation Force Microscopy: Fourier Analysis

G. Haugstad
University of Minnesota, Minneapolis, MN, USA, haugs001@umn.edu

ABSTRACT

Fourier analysis of oscillating forces at a shear-modulated tip provides new insight into static-to-kinetic friction transitions (stiction). In addition to contrast in conventional friction force microscopy, layers of autophobically dewetted PVA films exhibit remarkable differences in stiction. These differences relate to strong adsorption of first layer to mica substrate and concomitant conformational arrest, as compared to bulk-like behavior in the second layer. The third Fourier harmonic is found to be a sensitive gauge to variable degrees of sliding as a function of both drive amplitude and normal load (tensile to compressive). For a nanoscale drive, it is discovered that a largely static contact at compressive loads becomes a largely sliding contact at tensile loads. This finding has implications for the analysis of shear modulation force microscopy of polymers in the context of contact mechanics models, and for studies under variable sample compliance (temperature or solvent induced).

Keywords: shear modulation, confinement, AFM, stiction, polyvinyl alcohol

1 INTRODUCTION

Oscillatory methods in scanning probe microscopy have enabled nanoscale tribology and rheology investigations on polymeric systems. Among these methods, shear modulation force microscopy has been used to probe phenomena such as the stick-to-slide transition [1], time-delayed viscoelastic response [2], and near-surface glass transition [3], all at the nanoscale. Advantages of shear over normal modulation include a much stiffer torsional spring constant (comparable to that of the analyzed material), a simplified analytical expression for contact stiffness (independent of contact mechanics model), and minimal normal motion under shear drive (whereas parasitic shear motion is unavoidable under normal drive because of cantilever tilt). The commonly adopted approach is to measure the dynamic torsional forces on the tip via amplitude and phase outputs of a lock-in amplifier [1-3], to quantify the response to sinusoidal, nanometer-scale shear oscillations (of sample or tip). Missing in this approach are the details of real-time response that may reveal nonlinear interactions: strongly anharmonic distortions due to sliding, plastic yield or intrinsically nonlinear responses (e.g., nonlinear viscoelasticity, shear thinning). Given that fundamental polymeric responses are being studied, it is imperative to understand shear modulation phenomenology at a fundamental level. To this end we have examined nonlinear dynamic behavior under shear modulation via Fourier analysis of the real-time response. The methodology exploits the third harmonic of response as a gauge of nonlinearity due to partial sliding [4].

2 EXPERIMENTAL DETAILS

2.1 Materials.

Atactic polyvinyl alcohol (Aldrich, 99% hydrolyzed, Mw=85,000-146,000) was dissolved in distilled/deionized water at 1 wt% concentration by heating to 90° C for two hours under stirring, then diluted to 10^{-3} wt% and cast onto freshly cleaved, muscovite mica from a droplet as the water slowly evaporated over several hours. High-force scanning abrasion revealed a variable film thickness of approximately 1-5 nm depending on surface location.

2.2 Scanning probe microcopy.

Nanoscope III/Multimode (Digital Instruments) PicoScan/PicoSPM (Molecular Imaging) scanning probe microscopes (SPMs) were operated in contact mode in ambient conditions for general purpose imaging, and the latter was employed for shear-modulation protocols. The X-modulation signal (100-500 Hz, 5-500 mV amplitude sinusoidal corresponding to 0.25-25 nm X movement) was generated by a NI-6110E I/O card (National Instruments) controlled by LabView, or by a Hewlett Packard 33120A, then added to the X scanning signal from the PicoScan with a home-built circuit. During some measurements, scanning across the surface was one-dimensional (Y) and the "scan frequency" setting for X determined the sampling frequency; data were acquired such that the "X" dimension of "images" was instead the time dimension. In other measurements during 1-second approach-retract Z cycles ("force curves") at point locations, both normal cantilever deflection and torsion (shear force) in raw units of volts were measured and the data processed in two ways: (1) calculating the root-mean-square deviation of torsion per period of cycling and tabulating against the average normal deflection; (2) parsing the torsional data into five-period subintervals and fast Fourier transforming each subinterval. Shear modulation measurements utilized a single diving-board shaped, uncoated silicon cantilever with nominal spring constant of 3 N/m and nominal tip radius of curvature of 10 nm (Nanosensors). Approach-retract curves extended to a maximum load of ≈10 nN. Y-scanned measurements were performed under constant applied loads of 10-20 nN.

3 RESULTS AND DISCUSSION

PVA films prepared as described above contained a complex of holes, exemplified in the 20x20 μm height image of Figure 1a. The holes were roughly one to several microns across, and 3-4 nm deep. Corresponding strong contrast in sliding friction force was observed, with lower friction force inside of holes (lower surface elevations). This was quantitatively probed by acquiring lateral force images during both trace (left-to-right) and retrace (right-to-left), then subtracting the two images following a several-pixel offset of X to account for piezoscanner hysteresis. The resulting "friction loop" image is shown in Figure 1b. The friction image is dominated by two principal levels of friction force, within holes (lower friction force) and outside of holes (higher friction force). The ratio of mean friction force is 2.0, meaning the higher topographic regions are twice as dissipative as the lower regions within the holes.

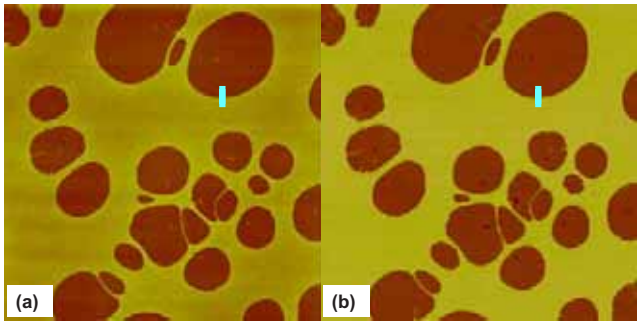

Figure 1. Topography (a) and friction-loop magnitude (b) images (20x20 μm) on an autophobically dewetted PVA film. Small vertical bars in (a) and (b) depict a typical domain for Y-scanned shear-modulation measurements.

High-force SPM scratching procedures at increasing loads sequentially revealed the selective removal of the higher surface regions, and ultimately the removal of a 1-nm thick first layer completely covering the substrate. These results indicate that *autophobic* dewetting, the phenomenon of a (usually polar) liquid not spreading on its own monolayer [5], occurred during film preparation. The reduction in sliding friction on the substrate-adsorbed layer ("Layer #1") is not as significant as found on highly crystalline microdomains (where chain packing strongly reduces dissipative motions) as characterized in other studies [6], but nonetheless implies reduced molecular freedom due to strong adsorption to substrate. The ultrathin geometry of this layer relative to the radius of gyration in the bulk (16.5 ± 2.5 nm) implies a high molecular asphericity, consistent with the strong polar interaction with mica. It is known that under strong substrate interaction, adsorbed chains have flattened, almost two-dimensional configurations. It is also theoretically expected that the substrate-adsorbed chains form a repulsive surface for chains not adsorbed to substrate, depleting chain density immediately atop the substrate-adsorbed layer (bright regions in Figure 1, "Layer 2"). These structural differences strongly impact dynamics, manifest here as differences in frictional response [7].

Time-dependent shear-modulated force response on Layers #1-2 was measured during Y-scanning of a small region as depicted in Figure 1, and over a set of drive amplitudes spanning from 0.25 nm to 25 nm. The results were Fourier analyzed and ratio of third to first harmonic calculated, as a gauge of nonlinearity due to partial sliding [4]. This ratio is plotted in Figure 2 as measured on Layer #1 and Layer #2. Each value derives from ≈10,000 analyzed cycles. An inflection point in A_3/A_1 is reached at drive amplitude of 1-2 nm on Layer #1 and 3-4 nm on Layer #2. It is within these intervals of drive amplitude that a characteristic transition from static- to kinetic-dominated friction takes place (static friction being significantly higher than kinetic friction). Above about 7-nm drive amplitude the ratio A_3/A_1 is surprisingly greater on Layer #2, albeit large in both cases signifying dominant sliding.

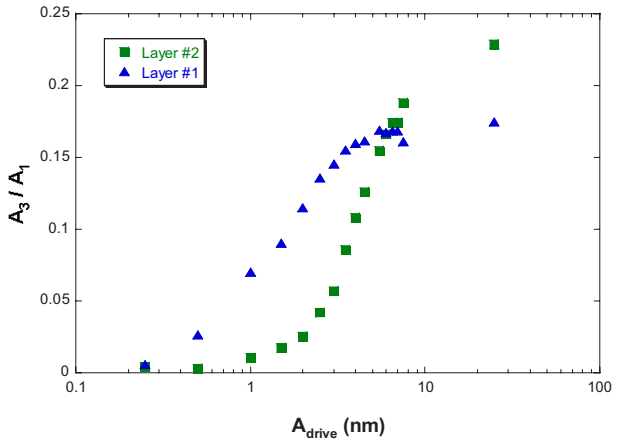

Figure 2. Fourier analysis of shear modulation measurements acquired over a set of drive amplitudes A_{drive} spanning from 0.25 nm to 25 nm. Plotted values are the ratio of the amplitudes of third to first harmonic, A_3/A_1.

That the transition from static to kinetic friction takes place at approximately 2:1 values of drive amplitude is highly suggestive. This finding implies that the differences of conformational mobility underlying a 2:1 ratio of static friction, or resistance to the onset of sliding, also result in a 2:1 ratio of kinetic or sliding friction. In turn this suggests that the ensemble of viscoelastic relaxations that comprise the sliding friction force [6] is similar to the ensemble of irreversible activation barriers that in aggregate must be overcome to initiate sliding.

Other measurements that help to assess stick-to-slide transitions, including the role of load, were obtained during approach-retract cycles. We present these results in Figure 3 in part to illustrate how our results relate to shear-modulation point measurements reported by others. The time dependence of shear and normal forces during an

approach-retract cycle, as implemented by Wahl et al. [8], is shown.

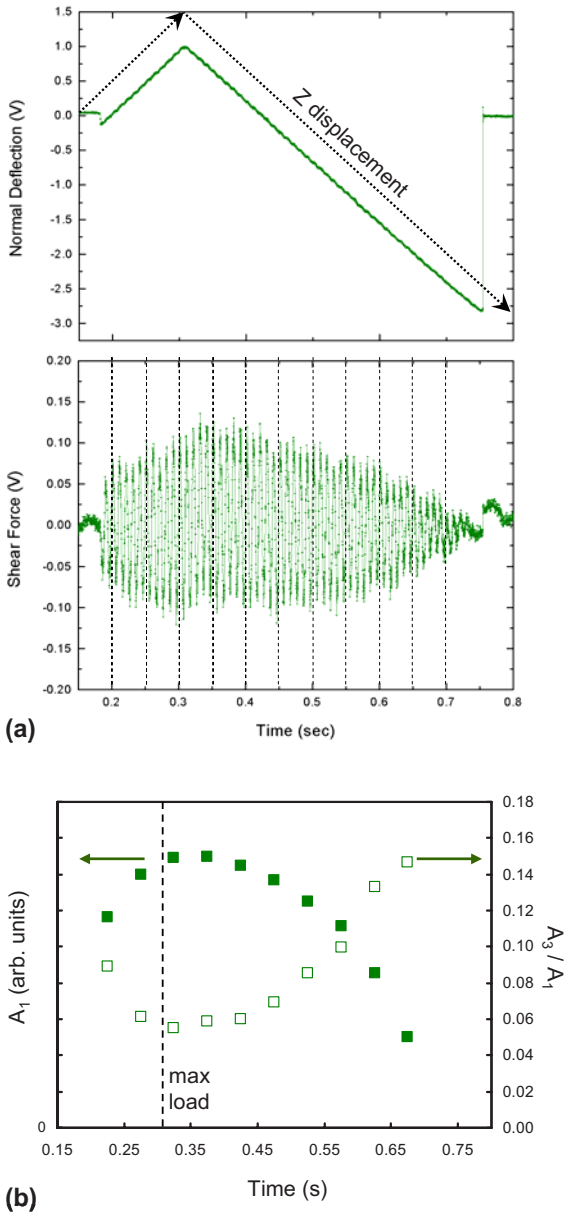

Figure 3. Time-domain response during an approach-retract cycle at a point on Layer #2. (a) Top: Vertical cantilever deflection (solid curve) with Z piezoscanner ramping motion depicted by dotted arrows. Bottom: Corresponding shear force response to sinusoidal X-displacement, subdivided into five-cycle time intervals for Fourier analysis. (b) Amplitude of first harmonic A_1 (closed squares) and ratio of amplitudes of third to first harmonic A_3/A_1 (open squares) determined from fast Fourier transforms of shear force response within each time interval denoted in bottom of (a).

Figure 3a contains representative raw shear force and normal (vertical) deflection signals acquired on Layer #2 under drive amplitude of 2.5 nm, spanning from compressive loads of ≈10 nN to tensile loads of ≈-30 nN just prior to pull-off. Figure 3b contains Fourier analysis of the shear force following the parsing of 50 oscillation periods into 10 subintervals as demarcated by vertical dashed lines in the lower graph of Figure 3a. The increase and subsequent decrease of the shear force amplitude that is apparent in Figure 3a (bottom) is more clearly represented by the plot of A_1 in Figure 3b. One finding is that the maximum in A_1 is reached later in time than the maximum in normal deflection (vertical dashed line) during Z ramping, as reported by Wahl et al. on polymeric systems [8] and attributed to the viscoelastic nature of tip-sample contact. A new finding in the present analysis is the corresponding evolution in A_3/A_1 seen during the approach-retract cycle: A_3/A_1 decreases to a minimum that coincides with the maximum in A_1, then increases up to break of adhesive contact in correspondence with a decrease in A_1. This result demonstrates, for the first time to our knowledge, that contact mechanics models may be naïve representations of what is actually occurring in many shear modulation studies on polymers (even if including viscoelasticity): a change from predominant stick to significant sliding depending on loading. Our results suggest that for many polymers, shear modulation measurements may be well-described by contact mechanics models only if the drive amplitude is in the sub-nanometer drive range, to study fixed contacts, or the tens-of-nanometer drive range to study sliding contacts.

Apart from the obvious difference of compression and tension, one also anticipates a change from weak stick under slight compression at low load (or low sample compliance) to strong stick under large compression at high load (or high sample compliance). Compliance-derived transitions may be induced for example by the glass-to-rubber transition whether temperature [3] or solvent (plasticization) induced.

Given that shear modulation microscopy studies generally have utilized the output of a lock-in amplifier, it is instructive to examine the load dependence of root-mean-squared (RMS) shear force response under 2.5-nm drive amplitude, Figure 4. Here each datum was computed from one cycle of real-time response, and is plotted versus the average value of vertical cantilever deflection (normal force, i.e. load) during the cycle. The data were collected during retraction from three point locations on each layer (triangles, Layer #1; squares, Layer #2). What is particularly notable on Layer #2 is the strong curvature of the data trends, compared to a nearly linear trend on Layer #1. Given the above identification of significant sliding under tension, we interpret the steep slope well into the tension regime (negative vertical deflections) as more characteristic of the coefficient of kinetic friction. The near-parallel nature of the data trends into the compressive regime (positive normal deflections) on both layers are

misleading, because the mechanisms of tip-sample interaction are very different on the two layers: mainly stick on Layer #2, whereas substantial sliding on Layer #1. The plot of RMS amplitude versus load on Layer 2 actually exhibits an approximate 1/3 power law as predicted by static contact mechanics models, even though Fourier analysis clearly indicates variable degrees of sliding. This suggests that the load dependence of RMS amplitude as conventionally measured with a lock-in amplifier may be misleading: one must definitively establish a stick condition before interpreting (fractional) exponents in the load dependence of shear modulation amplitude, or fitting this load dependence with functional forms predicted by contact mechanics models.

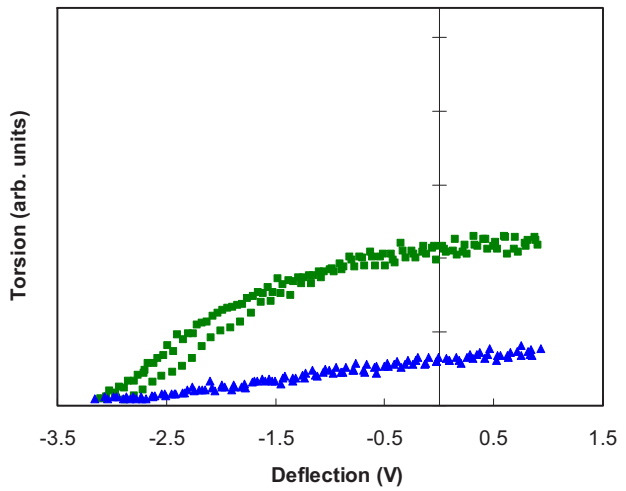

Figure 4. Root-mean-squared shear force response to sinusoidal shear displacement, versus vertical cantilever deflection during retraction from three locations on Layer #1 (triangles) and Layer #2 (squares) at 2.5-nm drive amplitude.

4 SUMMARY/CONCLUSIONS

Fourier analysis of spatially resolved, shear-modulated forces sheds new light on the transition from static to kinetic friction on polymers. The ratio of the amplitudes of third and first harmonic response is a sensitive gauge of the degree of sliding as a function of shear modulation amplitude. On autophobically dewetted polyvinyl alcohol film layers, this gauge identifies an approximate 2:1 ratio in the shear force needed to initiate sliding on second and first layers respectively, in correspondence with an approximate 2:1 ratio of sliding friction force as seen in conventional friction force microscopy. These differences apparently derive from conformational arrest in the strongly adsorbed first layer, as compared to more bulk-like mobility in the second layer.

Fourier analyzed response to a 2.5-nm shear modulated tip during approach-retract cycles reveals a change from a regime of primarily static friction at compressive loads of ≈10 nN to significant sliding at tensile loads of ≈-30 nN. This change of behavior impacts the functional relationship between RMS shear force response (as typically obtained with a lock-in amplifier) and applied load, rendering conventional contact mechanics models invalid. In using shear-modulated modes for mechanical and/or tribological studies, care should be exercised in choosing operating parameters so as to place the system in a well-defined regime (dominant stick or sliding), rather than a transitional regime where contrast interpretations and analytical modeling are problematic. More generally the interpretation of amplitude and/or phase images under variants of shear modulation including the recent "torsional resonance mode" [9] should be similarly impacted by the regime of operation.

REFERENCES

[1] H. –U. Krotil, E. Weilandt, Th. Stifter, O. Marti and S. Hild, Surf. Interface Anal. 27, 341, 1999.
[2] K. J. Wahl, S.V. Stepnow and W.N. Unertl, Trib. Lett. 5, 103, 1998.
[3] S. Ge, Y. Pu, W. Zhang, M. Rafailovich, J. Sokolov, C. Buenviaje, R. Buckmaster and R. M. Overney, Phys. Rev. Lett. 85, 2340, 2000.
[4] G. Haugstad, Trib. Lett. (in press).
[5] G. Reiter and R. Khanna, Langmuir 16, 6351, 2000.
[6] G. Haugstad, J.A. Hammerschmidt and W.L. Gladfelter, in Interfacial Properties on the Submicrometer Scale, J. Frommer and R.M. Overney, Editors. Oxford University Press: Washington, D.C (2001).
[7] J. Baschnagel, K. Binder, and A. Milchev, in Polymer Surfaces, Interfaces and Thin Films, A. Karim and S. Kumar, Editors. World Scientific Publishing: Singapore (2000).
[8] K. J. Wahl, S.V. Stepnowski and W.N. Unertl, Trib. Lett. 5, 103, 1998.
[9] T. Kasai et al., Nanotechnology 15, 731, 2004.